Biochemical and Biophysical Research Communications 408 (2011) 350–355

Contents lists available at ScienceDirect

Biochemical and Biophysical Research Communications

journal homepage: www.elsevier.com/locate/ybbrc

A multishear microfluidic device for quantitative analysis of calcium dynamics in osteoblasts

Songzi Kou [a], Leiting Pan [a,*], Danny van Noort [b], Guixian Meng [a], Xian Wu [a], Haiying Sun [a], Jingjun Xu [a], Imshik Lee [a,*]

[a] The Key Laboratory of Weak-Light Nonlinear Photonics, Ministry of Education, School of Physics and TEDA Applied Physics School, Nankai University, Tianjin 300457, China
[b] MechanoBiology Institute, Singapore, T-Lab, 5A Engineering Drive 1, National University of Singapore, Singapore 117411, Singapore

ARTICLE INFO

Article history:
Received 24 March 2011
Available online 13 April 2011

Keywords:
Microfluidics
Multishear device
Osteoblasts
Calcium dynamics

ABSTRACT

Microfluidics is a convenient platform to study the influences of fluid shear stress on calcium dynamics. Fluidic shear stress has been proven to affect bone cell functions and remodelling. We have developed a microfluidic system which can generate four shear flows in one device as a means to study cytosolic calcium concentration ($[Ca^{2+}]_c$) dynamics of osteoblasts. Four shear forces were achieved by having four cell culture chambers with different widths while resistance correction channels compensated for the overall resistance to allow equal flow distribution towards the chambers. Computational simulation of the local shear stress distribution highlighted the preferred section in the cell chamber to measure the calcium dynamics. Osteoblasts showed an $[Ca^{2+}]_c$ increment proportional to the intensity of the shear stress from 0.03 to 0.30 Pa. A delay in response was observed with an activation threshold between 0.03 and 0.06 Pa. With computational modelling, our microfluidic device can offer controllable multishear stresses and perform quantitative comparisons of shear stress-induced intensity change of calcium in osteoblasts.

1. Introduction

Shear stress induced by physical activities has been shown to modulate bone cell functions and bone maintenance [1,2]. To investigate bone cell functions *in vitro*, extracellular fluid flow was introduced to cells cultured in artificial fluid shear devices, making it possible to study the mechanosensing at subcellular level [3]. More specifically, fluid flow shear stress can induce intracellular calcium response and intercellular calcium signalling in bone cells [4]. As one of the second messengers, calcium is important for the proliferation, differentiation, apoptosis and metabolism of bone cells [5]. The cytosolic calcium concentration ($[Ca^{2+}]_c$) is regulated by controlling calcium release from intracellular calcium stores or calcium influx [6]. Many flow studies have demonstrated that bone cells, such as osteoblasts or osteoblast-like cells [7–14], osteocytes [15,16] and chondrocytes [17], exhibit a $[Ca^{2+}]_c$ response under various fluid shear stress conditions. In these studies, a parallel-plate flow chamber [18] or derivative devices have been mostly used as the fluid shear stress generating devices. However, these devices have their inherent drawbacks, including variability in device thickness and complication in assembly processes. Another drawback is that devices such as the parallel plate or other on-chip [19–21] calcium influx assays cannot generate multiple shear stresses simultaneously.

To systematically study calcium dynamics, microfluidic devices allow for easy control of the physicochemical microenvironment, while using small amounts of reagents [22]. Because of the similar dimensions as biological structures, microfluidic based cell cultures mimic the *in vivo* extracellular microenvironment more closely than other devices [23]. Multishear microfluidic devices have been used to analyze cell adhesion [24,25], cell mechanics [26] and cell proliferation [27]. However, there has been no previous work on the measurement of $[Ca^{2+}]_c$ for osteoblasts in a multishear microfluidic device. Therefore, to evaluate the dynamics of $[Ca^{2+}]_c$ in real time, we designed a multishear microfluidic device that allowed controlled fluidic shear stress on osteoblasts in parallel. This device consisted of four cell-culture chambers with balanced resistance by resistance correction channels before and after the chambers. The local shear stress distribution in each chamber was computationally simulated and the region with uniform shear stress in these chambers was determined. Only cells in these uniform shear stress regions were chosen for $[Ca^{2+}]_c$ measurement. The results showed that the cells exposed to flow shear stress demonstrated $[Ca^{2+}]_c$ increment which was dependent on the shear stress intensity. The calcium response showed similar behaviour for all the stresses. A delay in response was observed at the activation threshold of 0.03 Pa.

* Corresponding authors. Fax: +86 22 66229310.
E-mail addresses: plt@nankai.edu.cn (L. Pan), ilee@nankai.edu.cn (I. Lee).

0006-291X/$ - see front matter © 2011 Elsevier Inc. All rights reserved.
doi:10.1016/j.bbrc.2011.04.044

2. Materials and methods

2.1. Cell isolation and culture

Osteoblasts isolation and culture method was described in our earlier work [28,29]. Cells were cultured in DMEM (Gibco, Gland Island, NY, USA) that was supplemented with 15% FBS (Lanzhou National Hyclone Bio-engineering Co., Ltd., Lanzhou, China) and 100 U penicillin + 100 μg/mL streptomycin (Gibco, USA). 0.25% trypsin–EDTA (Gibco, USA) was used to digest cells. For the shear stress experiment, the cells in passage 4–6 were inoculated in microfluidic channels and were cultured overnight.

2.2. Device design and fabrication

The mask was designed in AutoCAD (San Rafael, CA, USA) and was printed on high-resolution transparency films (CAD/Art Services, Inc., IL, USA). The dimensions of resistance channels were 200 μm × 160 μm (width × height). The master mold was made by spinning a layer (approx. 160 μm) of negative photoresist SU-8 2150 (500 rpm, 10 s; 3000 rpm, 30 s) on a 4″ silicon wafer (Single Crystal Substrates of America, Inc., IL, USA) and soft baking them in two steps on a hotplate (65 °C, 5 min; 95 °C, 50 min). After cooling, the photoresist was exposed via a transparency mask for 2 min using a manual mask aligner (SUSS MicroTec Lithography GmbH, Germany) and postbaked (65 °C 5 min; 95 °C, 15 min). After being developed for 10–15 min, the molds were treated with trimethylchlorosilane (United Chemical Technologies, Inc., Bristol, PA, USA) vapour in vacuum for 15 min to facilitate mold release. The fabrication process of PDMS chips has been described previously [30].

2.3. Computational simulation of wall shear stress

The three-dimensional flow in the microfluidic channel was modelled using FLUENT 6.5 software (ANSYS, Inc., Lebanon, NH, USA). Simulations were conducted for 400, 800, 1600 and 3200 μm wide cell culture chambers. The three-dimensional chamber models were designed in AutoCAD and were then meshed in GAMBIT (ANSYS, Inc.) with 78,000 nodes. The computations were performed under the assumption that the flow was laminar and steady. The density of DMEM medium, which was used as the perfusate, is 993.2 kg/m^3 and its viscosity is 7.85 × 10^{-4} kg/m s at 37 °C.

2.4. Cell inoculation in the microfluidic chambers

The microfluidic device was sterilized in an autoclave (G154D, Zealway Instrument, Inc., USA) and then air-dried on a clean bench. The cell culture chambers were filled with 0.01% poly-L-lysine (Sigma, USA) and left for 1 h at room temperature to form a coating. After coating, the chambers were washed with sterilized water. A suspension of cells at passages 4–6 was prepared at a concentration of 8 × 10^5 cells/mL and was introduced into the device by pushing the cells slowly into the culture chambers with a 1-mL syringe (Shanghai Zhiyu Medical Material Co., Ltd., Shanghai, China) at the outlets of the microfluidic device. The device with cells was incubated at 37 °C in 5% CO_2 overnight to allow cell attachment.

2.5. Cell staining

The cytosolic calcium concentration was measured using a calcium indicator, fluo-3 AM (Invitrogen Co., Eugene, OR, USA). DMEM medium was washed out of the microchannels using HBSS buffer (8.182 g/L NaCl, 0.374 g/L KCl, 0.111 g/L $CaCl_2$, 0.203 g/L $MgCl_2{\cdot}6H_2O$, 2.383 g/L HEPES, 1.983 g/L glucose, pH 7.4). Then, 5 μM fluo-3 was loaded into the microfluidic cell culture chambers and incubated with cells for 30 min at 37 °C. Nonspecifically associated dyes were removed by washing the microchannels with HBSS. Cells were incubated for a further 30 min to allow complete de-esterification of intracellular AM esters.

2.6. System setup and data analysis

The imaging system was used as described previously [31]. Briefly, the microfluidic device was mounted on an inverted fluorescence microscope (Carl Zeiss, Germany) with a 100 W mercury lamp as the light source. A filter set with an excitation filter (487 nm), dichroic mirror (505 nm), emission filter (530 nm) and a Fluar 40×/1.30 oil immersion objective lens was used. An electron-multiplying charge-coupled device (DU-897D, Andor, UK) and MetaMorph 7.1 software (Universal Imaging Corp., Downingtown, PA, USA) was used to analyze the fluorescence intensity of individual cells. The flow rates were controlled by a peristaltic pump (BT00-300M-YZ1515X, Baoding Longer Precision Pump Co., Ltd., Hebei, China). For all measurements, the background fluorescence intensity was subtracted using the intensity of an adjacent cell-free region. The baseline fluorescence intensity was taken as an average initial value over 20 s before applying either shear stress.

3. Results

3.1. Multishear microfluidic device design

Fig. 1A and B shows the overview of the multishear microfluidic device for measuring $[Ca^{2+}]_c$ of osteoblasts. The device consists of one inlet and four separate branches. Each branch includes two sets of winding channels, one cell culture chamber and one outlet. The inlet was used to introduce reagents into the device. The resistance channels were used to stabilize and equalize the flow distribution. The outlet was used for collecting waste and seeding cells into the chambers.

For a steady-state pressure-driven flow in rectangular microchannels [32], the fluidic resistance, R, is the function of the channel width, w, the channel height, h, the viscosity, μ and the channel length, L, as follows,

$$R = \frac{12\mu L}{wh^3}\left[1 - \frac{h}{w}\left(\frac{192}{\pi}\sum_{n=1,3,5}^{\infty}\frac{1}{n^5}\tanh\left(\frac{n\pi w}{2h}\right)\right)\right]^{-1} \quad (1)$$

The resistance ratio between the resistance channels (R_r) and the cell culture chamber (R_c) in each branch were 18:1, 41:1, 88:1 and 183:1. As $R_r >> R_c$, the flows could be considered as being equally distributed to each cell culture chamber.

The chambers had the same length (5400 μm) but different widths: 3200, 1600, 800 and 400 μm, producing four different flow velocities and, therefore, four different fluid shear stress profiles. The shear stress-stimulating system was accomplished by connecting the microfluidic device to a peristaltic pump via silicone and PE tubing (Fig. 1C). The flow of reagents collected during a certain period of time gave the flow rate in μL/min. In further reference, the cell culture chambers are indicated as: chamber 1 (Ch_1), chamber 2 (Ch_2), chamber 3 (Ch_3) and chamber 4 (Ch_4).

3.2. Computational simulation of the wall shear stress distribution in cell culture chambers

Pressure-driven flow through rectangular channels is a well-known phenomenon. The flow through the cell culture chamber was modelled as a *Poiseuille* flow. The fluid shear stress on the cells was assumed to be equal to the shear stress at the wall. Fig. 2A

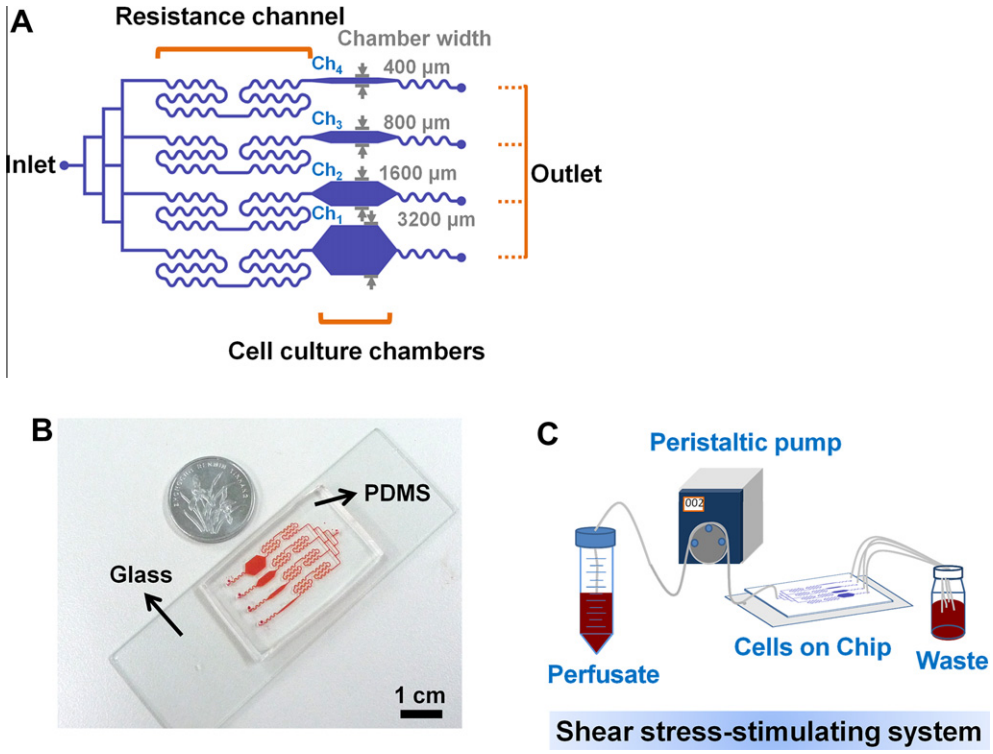

Fig. 1. Microfluidic shear device overview. (A) A schematic view of the device design. The chambers (from bottom to top) are indicated as Ch_1, Ch_2, Ch_3 and Ch_4. The chamber widths are 3200, 1600, 800, 400 μm. (B) A device pictured next to a Chinese 0.1 yuan coin for illustrative purpose. The chip was filled with red food dye. (C) A schematic illustration of the shear stress-stimulating system.

shows the simulation results of the wall shear stress distribution depicted as contours in each chamber. A region with uniform shear stress was found in the central part of each chamber. Only at the edges and corners of the chamber were there sharp changes in the uniformity. To quantify the local distribution of the shear stress, we computed the shear stress along the vertical and horizontal center axis of the cell chamber. The center of each chamber was chosen as the origin (0,0) (Fig. 2B and C). Along the vertical axis, the uniform shear stress was in the region (0, −1000) to (0, 1000) for each chamber, with a total distance of 2000 μm. Along the horizontal axis, the uniform shear stress was in the regions (−1250, 0) to (1250, 0), (−500, 0) to (500, 0), (−200, 0) to (200, 0) and (−100, 0) to (100, 0) with a total distance of 2500, 1000, 400 and 200 μm for Ch_1, Ch_2, Ch_3 and Ch_4, respectively. When using a flow rate of 31 μL/min, the resultant shear stress values in these uniform regions were 0.03, 0.06, 0.13 and 0.30 Pa for Ch_1, Ch_2, Ch_3 and Ch_4.

3.3. Phenomenon of cytosolic calcium levels with varying shear stresses in microfluidic chambers

After being cultured overnight in the microfluidic cell culture chambers, the osteoblasts were attached to the poly-L-lysine-coated glass surface. Only cells in the uniform shear stress region were imaged using fluorescence microscopy. Representative real-time fluorescent images of cells at different time points are shown in Fig. 3. The perfusate used was a cell culture medium, DMEM. The observed cells showed increased fluorescence intensity after the start of the flow, meaning an increase in $[Ca^{2+}]_c$. Approximately 6–7 live cells were quantified at each shear condition, and each experiment was repeated three times.

3.4. Quantitative analysis of cytosolic calcium response under different shear stresses

$[Ca^{2+}]_c$ profiles are shown in Fig. 4A–D by measuring the changes in fluorescence intensity under a flow stimulation for 2 min. These profiles show three distinctive features of $[Ca^{2+}]_c$: peak, stability and recovery. The peak corresponded to the start of the mechanotransduction signal. The stable signal presented physiological equilibrium while under stress. After switching off the flow, the $[Ca^{2+}]_c$ dropped back to their initial values. Clearly the $[Ca^{2+}]_c$ increase depended on the shear stress intensity. Higher shear stress induced a greater calcium increase in some cells. Statistical data analysis showed that the means of the $[Ca^{2+}]_c$ peak values were proportional to the intensity of the shear stress (Fig. 4E). The mean baseline $[Ca^{2+}]_c$ level before flow was normalized to 1. The average of peak $[Ca^{2+}]_c$ response values for the four shear stresses (from low to high) were 1.74 ± 0.31, 2.78 ± 0.50, 3.20 ± 0.56 and 4.04 ± 0.75. In contrast to the means of the peak $[Ca^{2+}]_c$ response values, the response time (the time from the start of the flow to the peak $[Ca^{2+}]_c$ response) was independent of the shear stress for values larger than 0.03 Pa (Fig. 4F). Only the response time at 0.03 Pa, which was 19.75 ± 8.85 s, showed a significant difference from that of the other three shear stresses. The response times at 0.06, 0.12 and 0.24 Pa shear stresses were 10.07 ± 2.00 s, 10.56 ± 2.35 s and 9.52 ± 1.89 s, showing no significant difference. This result could mean that a stress larger than 0.03 Pa is needed to elicit calcium mobilization.

4. Discussion

The overall aim of this work was to assess the potential use of a multishear microfluidic device to study calcium dynamics in cells under controlled shear stress conditions. The device was fabricated

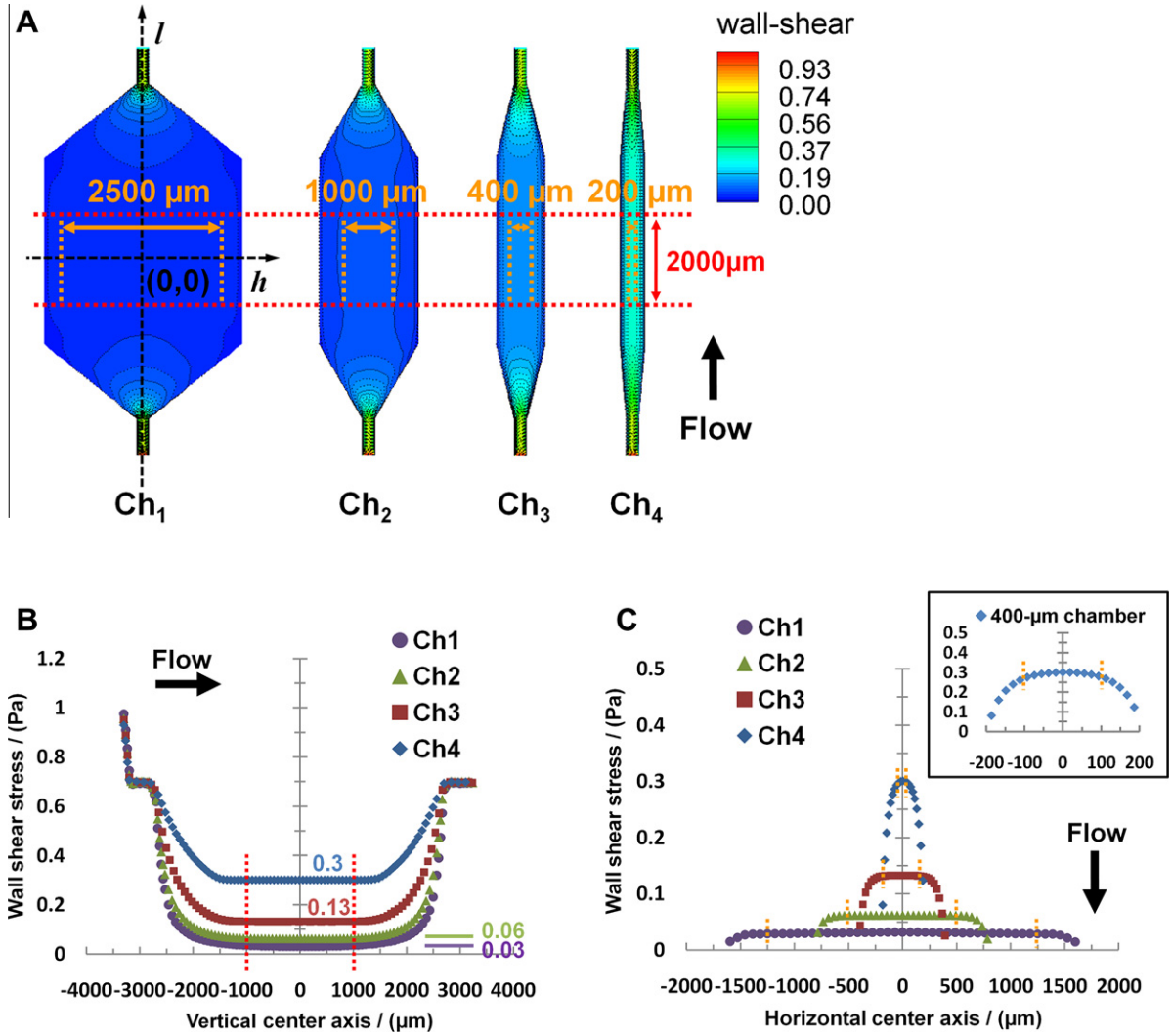

Fig. 2. Computational simulation of wall shear stress distribution in cell culture chambers. (A) Contours of wall shear stress distribution in designed chambers. From left to right, central areas of each chamber, 2500 μm × 2000 μm, 1000 μm × 2000 μm, 800 μm × 2000 μm and 400 μm × 2000 μm (horizontal distance × vertical distance), showed uniform wall shear stress at the flow rate of 31 μL/min. The uniform wall shear stress area boundary was indicated by orange and red dashed line. (B) Wall shear stress profiles along the vertical center axis (v) and (C) horizontal center axis (h). (For interpretation of the references to colour in this figure legend, the reader is referred to the web version of this article.)

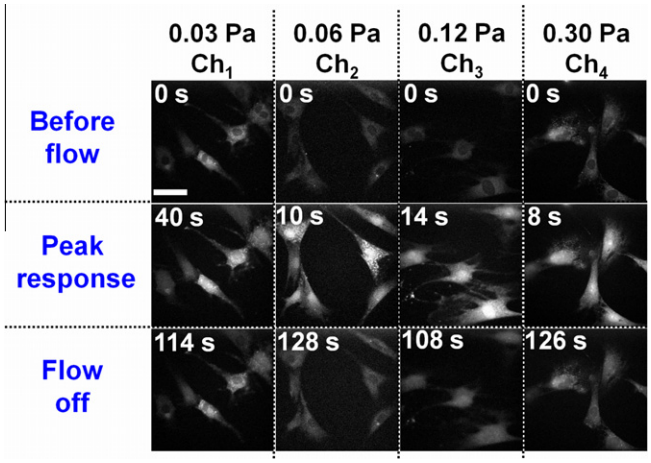

Fig. 3. $[Ca^{2+}]_c$ microscopy measurements. Representative time-series fluorescent images of cells before flow, on peak response and flow off, corresponding to cells in Ch_1, Ch_2, Ch_3 and Ch_4 (0.03, 0.06, 0.13 and 0.30 Pa), The 2 min continuous shear stimulation elicited a heterogeneous calcium increase. The scale bar is 20 μm.

using standard soft-lithography [33]. To measure calcium response of osteoblasts to fluid flow, *in vitro* experiments are generally performed in parallel-plate flow chambers or similar devices. Some advances have already been made in measuring $[Ca^{2+}]_c$ in microfluidics, however using different cell types [19–21,34,35]. Compared to these devices, our microfluidic device has the following advantages: multiple shear stresses in one device, easy assembly, easy read-out of calcium dynamics, readily sterilized using common procedures, such as autoclaving or ethanol treatment.

For our multishear device, we introduced a network of fluidic resistance channels based on numerical solutions of the laminar flow in a confined channel (Fig. 1A and B). The network included two sets of winding channels serving as resistance correction channels. The resistance of these channels was much larger than that of the cell culture chamber in each branch. This allowed for equal flow distribution for four branches. Different shear stresses could then be achieved by changing the width of the cell chamber. In the shear stress-stimulating system, the flow rate was simply adjusted by a peristaltic pump, which was then hermetically connected to the microfluidic device by tubing (Fig. 1C). To estimate the shear stress, we performed a computational simulation on

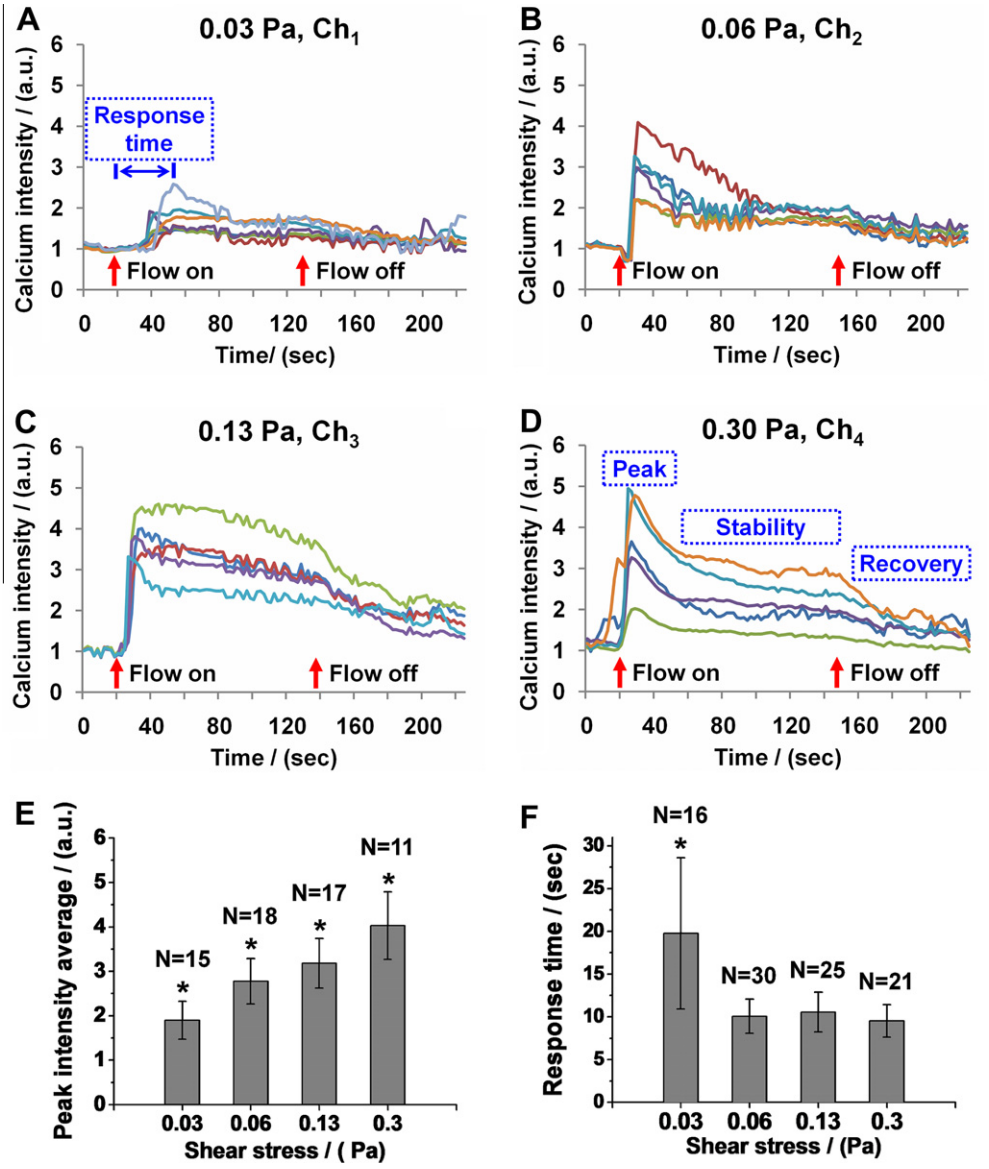

Fig. 4. Calcium profiles and quantitative analysis of cytosolic calcium response. (A–D) Representative profiles of single cell response under four shear conditions. Flow on and off time are indicated with red arrows. Response time was defined as the time from the start of the flow to the peak $[Ca^{2+}]_c$ response. The profiles show three distinctive features of $[Ca^{2+}]_c$ peak, stability and recovery. (E) Stress dependent peak calcium response. (F) Calcium response time versus different shear stresses. The data shown represents the mean ± SD. *Indicates statistical significance between shear stress levels ($P < 0.05$). (For interpretation of the references to colour in this figure legend, the reader is referred to the web version of this article.)

the local shear stress distribution of the cell culture chamber. The results showed a uniform shear stress region in each chamber. As shown in Fig. 2, the proportion of uniform shear stress area to the whole chamber area decreased for decreasing chamber width. The resultant shear stress values in these uniform regions were 0.03, 0.06, 0.13 and 0.30 Pa for Ch_1, Ch_2, Ch_3 and Ch_4, at a flow rate of 31 μL/min.

The performance of device was investigated by comparing the $[Ca^{2+}]_c$ dynamics under varying shear stress in each chamber. Osteoblasts showed an $[Ca^{2+}]_c$ incremental response under shear stress stimulation (Fig. 3). Cells displayed similar characteristic $[Ca^{2+}]_c$ profiles to different shear stresses (Fig. 4A–D). These profiles can be divided into three sections. First, the $[Ca^{2+}]_c$ peak signal was caused by the activation of the mechanotransduction at the start of the flow [36]. But this increase was counter-regulated by the cell to prevent excessive calcium influx. Second, the competing effect of shear stimulation and the cell's self-regulation caused the stable signal in the calcium response. Third, once the flow, and therefore the shear stress, was stopped, $[Ca^{2+}]_c$ tended to recover to their original state. The stable signal showed a duration increase with the increasing of shear stress. For a quantitative comparison between $[Ca^{2+}]_c$ dynamics under each shear stress, analysis shows that the peak $[Ca^{2+}]_c$ response values are dependent on the fluid shear stress intensity, the higher the shear stress the greater the $[Ca^{2+}]_c$ increase, which is consistent with findings of previous studies [7,9,11]. Fig. 4F shows that the response time of $[Ca^{2+}]_c$ signals is delayed at the onset of the shear flow. At the lowest shear stress of 0.03 Pa, the responding delay was 19.75 ± 8.85 s, while for stresses larger than 0.06 Pa, this delay was approximately 10 s. The existence of an activation threshold of the applied shear stress has previously been observed [7]. In our measurements, the activation threshold of shear stress was shown to be between 0.03 and 0.06 Pa for osteoblasts.

In conclusion, we have developed a multishear microfluidic device which can generate controlled multiple shear stresses in one device for the measurement of $[Ca^{2+}]_c$ dynamics in osteoblasts.

The device was fabricated by using standard soft-lithography. Computational simulation estimated the shear stress values and highlighted a uniform region of shear stress. The device lent itself well to measure the $[Ca^{2+}]_c$ response of osteoblasts. Since microfluidic system is an emerging tool to study cell functional assay, we believe that our multishear device provides a valuable platform to quantitatively analyze shear stress effects on cells.

Acknowledgments

We would like to thank Prof. Kai Zhang for instructions on the shear stress computational simulations. This work was supported by National Natural Science Foundation of China (No. 11074133), the Fundamental Research Funds for the Central Universities (No. 65010861), the National Basic Research Program of China (No. 2007CB307002) and 111 Project (No. B07013).

References

[1] C.Y. Huang, R. Ogawa, Mechanotransduction in bone repair and regeneration, Faseb J. 24 (2010) 3625–3632.
[2] C.R. Jacobs, S. Temiyasathit, A.B. Castillo, Osteocyte Mechanobiology and Pericellular Mechanics, Annual Review of Biomedical Engineering, vol. 12, Annual Reviews, Palo Alto, 2010, pp. 369–400.
[3] R.C. Riddle, H.J. Donahue, From streaming potentials to shear stress: 25 years of bone cell mechanotransduction, J. Orthop. Res. 27 (2009) 143–149.
[4] J. Rubin, C. Rubin, C.R. Jacobs, Molecular pathways mediating mechanical signaling in bone, Gene 367 (2006) 1–16.
[5] D.J. Papachristou, K.K. Papachroni, E.K. Basdra, A.G. Papavassiliou, Signaling networks and transcription factors regulating mechanotransduction in bone, Bioessays 31 (2009) 794–804.
[6] C.W. Taylor, Controlling calcium entry, Cell 111 (2002) 767–769.
[7] F.D. Allen, C.T. Hung, S.R. Pollack, C.T. Brighton, Serum modulates the intracellular calcium response of primary cultured bone cells to shear flow, J. Biomech. 33 (2000) 1585–1591.
[8] C.T. Hung, F.D. Allen, S.R. Pollack, C.T. Brighton, Intracellular Ca^{2+} stores and extracellular Ca^{2+} are required in the real-time Ca^{2+} response of bone cells experiencing fluid flow, J. Biomech. 29 (1996) 1411–1417.
[9] C.T. Hung, S.R. Pollack, T.M. Reilly, C.T. Brighton, Real-time calcium response of cultured bone cells to fluid flow, Clin. Orthop. Relat. Res. 00 (1995) 256–269.
[10] B. Huo, X.L. Lu, C.T. Hung, K.D. Costa, Q.B. Xu, G.M. Whitesides, X.E. Guo, Fluid flow induced calcium response in bone cell network, Cell Mol. Bioeng. 1 (2008) 58–66.
[11] C.R. Jacobs, C.E. Yellowley, B.R. Davis, Z. Zhou, J.M. Cimbala, H.J. Donahue, Differential effect of steady versus oscillating flow on bone cells, J. Biomech. 31 (1998) 969–976.
[12] N.N. Batra, Y.J. Li, C.E. Yellowley, L.D. You, A.M. Malone, C.H. Kim, C.R. Jacobs, Effects of short-term recovery periods on fluid-induced signaling in osteoblastic cells, J. Biomech. 38 (2005) 1909–1917.
[13] N.X. Chen, K.D. Ryder, F.M. Pavalko, C.H. Turner, D.B. Burr, J.Y. Qiu, R.L. Duncan, Ca^{2+} regulates fluid shear-induced cytoskeletal reorganization and gene expression in osteoblasts, Am. J. Physiol. – Cell Physiol. 278 (2000) C989–C997.
[14] S.W. Donahue, H.J. Donahue, C.R. Jacobs, Osteoblastic cells have refractory periods for fluid-flow-induced intracellular calcium oscillations for short bouts of flow and display multiple low-magnitude oscillations during long-term flow, J. Biomech. 36 (2003) 35–43.
[15] C. Liu, Y. Zhao, W.Y. Cheung, R. Gandhi, L.Y. Wang, L.D. You, Effects of cyclic hydraulic pressure on osteocytes, Bone 46 (2010) 1449–1456.
[16] H. Kamioka, Y. Sugawara, S.A. Murshid, Y. Ishihara, T. Honjo, T. Takano-Yamamoto, Fluid shear stress induces less calcium response in a single primary osteocyte than in a single osteoblast: implication of different focal adhesion formation, J. Bone Miner. Res. 21 (2006) 1012–1021.
[17] G.R. Erickson, L.G. Alexopoulos, F. Guilak, Hyper-osmotic stress induces volume change and calcium transients in chondrocytes by transmembrane, phospholipid, and G-protein pathways, J. Biomech. 34 (2001) 1527–1535.
[18] J.A. Frangos, S.G. Eskin, L.V. McIntire, C.L. Ives, Flow effects on prostacyclin production by cultured human endothelial cells, Science 227 (1985) 1477–1479.
[19] X.L. Zhang, H.B. Yin, J.M. Cooper, S.J. Haswell, A microfluidic-based system for analysis of single cells based on Ca^{2+} flux, Electrophoresis 27 (2006) 5093–5100.
[20] H.B. Yin, X.L. Zhang, N. Pattrick, N. Klauke, H.C. Cordingley, S.J. Haswell, J.M. Cooper, Influence of hydrodynamic conditions on quantitative cellular assays in microfluidic systems, Anal. Chem. 79 (2007) 7139–7144.
[21] A.R. Wheeler, W.R. Throndset, R.J. Whelan, A.M. Leach, R.N. Zare, Y.H. Liao, K. Farrell, I.D. Manger, A. Daridon, Microfluidic device for single-cell analysis, Anal. Chem. 75 (2003) 3581–3586.
[22] D. van Noort, S.M. Ong, C. Zhang, S.F. Zhang, T. Arooz, H. Yu, Stem Cells in microfluidics, Biotechnol. Progr. 25 (2009) 52–60.
[23] Y.C. Toh, C. Zhang, J. Zhang, Y.M. Khong, S. Chang, V.D. Samper, D. van Noort, D.W. Hutmacher, H.R. Yu, A novel 3D mammalian cell perfusion-culture system in microfluidic channels, Lab Chip 7 (2007) 302–309.
[24] E. Gutierrez, B.G. Petrich, S.J. Shattil, M.H. Ginsberg, A. Groisman, A. Kasirer-Friede, Microfluidic devices for studies of shear-dependent platelet adhesion, Lab Chip 8 (2008) 1486–1495.
[25] H. Lu, L.Y. Koo, W.C.M. Wang, D.A. Lauffenburger, L.G. Griffith, K.F. Jensen, Microfluidic shear devices for quantitative analysis of cell adhesion, Anal. Chem. 76 (2004) 5257–5264.
[26] L. Chau, M. Doran, J. Cooper-White, A novel multishear microdevice for studying cell mechanics, Lab Chip 9 (2009) 1897–1902.
[27] L. Kim, M.D. Vahey, H.Y. Lee, J. Voldman, Microfluidic arrays for logarithmically perfused embryonic stem cell culture, Lab Chip 6 (2006) 394–406.
[28 X.L. Liu, X. Zhang, I. Lee, A quantitative study on morphological responses of osteoblastic cells to fluid shear stress, Acta. Biochem. Biophys. Sin. 42 (2010) 195–201.
[29] X. Zhang, X.L. Liu, J.L. Sun, S.J. He, I. Lee, H.K. Pak, Real-time observations of mechanical stimulus-induced enhancements of mechanical properties in osteoblast cells, Ultramicroscopy 108 (2008) 1338–1341.
[30] S.Z. Kou, H.N. Lee, D. van Noort, K.M.K. Swamy, S.H. Kim, J.H. Soh, K.M. Lee, S.W. Nam, J. Yoon, S. Park, Fluorescent molecular logic gates using microfluidic devices, Angew. Chem. Int. Edit. 47 (2008) 872–876.
[31] L.T. Pan, X.Z. Zhang, K. Song, X. Wu, J.J. Xu, Exogenous nitric oxide-induced release of calcium from intracellular IP3 receptor-sensitive stores via S-nitrosylation in respiratory burst-dependent neutrophils, Biochem. Biophys. Res. Co. 377 (2008) 1320–1325.
[32] D.J. Beebe, G.A. Mensing, G.M. Walker, Physics and applications of microfluidics in biology, Annu. Rev. Biomed. Eng. 4 (2002) 261–286.
[33] Y.N. Xia, G.M. Whitesides, Soft lithography, Annu. Rev. Mater. Sci. 28 (1998) 153–184.
[34] X.J. Li, P.C.H. Li, Microfluidic selection and retention of a single cardiac myocyte, on-chip dye loading, cell contraction by chemical stimulation, and quantitative fluorescent analysis of intracellular calcium, Anal. Chem. 77 (2005) 4315–4322.
[35] P.H.G. Chao, A.C. West, C.T. Hung, Chondrocyte intracellular calcium cytoskeletal organization, and gene expression responses to dynamic osmotic loading, Am. J. Physiol. – Cell Physiol. 291 (2006) C718–C725.
[36] M.J. Berridge, M.D. Bootman, H.L. Roderick, Calcium signalling: dynamics homeostasis and remodelling, Nat. Rev. Mol. Cell Biol. 4 (2003) 517–529.